J. Amr. Uni. ***03*** *(2023) p.109*

Tracking of Formed Crystalline Phases in the Binary Silver Tellurite Glass-ceramics

M. El Zaibani[a,*], A. Altawaf [b], E. F. El Agammy[c,*]
[a] Physics Department, Faculty of Education, Amran University, Amran, Yemen.
[b] Department of Physics, Faculty of Education, Hajjah University, Hajjah, Yemen.
[c] Physics Department, College of Science, Jouf University, P.O. Box: 2014, Sakaka, Saudi Arabia.

Abstract

Glasses and glass-ceramics based on silver tellurite system $x$$Ag_2O$·(100-$x$)$TeO_2$ ($0 \le x \le 60$ mol%) were prepared by melt-quenching method. The structure of the studied glasses and glass-ceramics was investigated by several techniques. XRD patterns reveal the existence of only one glassy region at $20 < x \le 30$ mol% with two crystalline α-TeO_2 and Ag_2TeO_3 phases that formed separately in the prepared samples below 20 and beyond 30 mol% Ag_2O, respectively. The peaks intensity corresponding to the crystalline α-TeO_2 and Ag_2TeO_3 phases was found to decrease and increase with Ag_2O content, respectively. This may be correlated with changes in the concentration of Q_4^4 and Q_3^0 units that, respectively, build up the crystalline α-TeO_2 and Ag_2TeO_3 phases. In the glassy region, there is no crystalline phase, which may be attributed to the abundance of the deformed Q_4^3 units that build up the glassy phase, and the concentrations of Q_4^4 and Q_3^0 units are neglected in this region. SEM and TEM micrographs and the related electron diffraction patterns (EDP) confirmed the formation of crystallized clusters in Ag_2O-rich glasses.

Keywords: Ag_2O-TeO_2 glasses and glass-ceramics; Ag_2O-rich TeO_2; Q_m^n unis; Clusters; Ag_2TeO_3 phase; α-TeO_2 phase; XRD; TEM and EDP techniques.

الملخص: الزجاج والزجاج–السيراميكي ذو الصيغة $xAg_2O.(100\text{-}x)TeO_2 (0 \le x \le 6 mol\%$ تم تحضيره بطريقة الصهر التقليدية. كما تم استخدام تقنيات عديده في دراسة تركيب العينات المدروس. تكشف انماط الاشعة السينية عن وجود منطقة زجاجية واحدة في $20 < x \le 30$ mol% مع طورين متبلورتين α–TeO_2 وAg_2TeO_3 والتي تشكلت بشكل منفصل في العينات المحضرة Ag_2O أقل من 20 وما بعد 30 مول٪، على التوالي. تم العثور على شدة القمم المقابلة للطورين α–TeO_2 وAg_2TeO_3 البلورية تتناقص وتزيد مع محتوى Ag_2O، على التوالي. هذا ربما مرتبط مع التغيرات في تركيز الوحدات التركيبية Q_4^4 و Q_3^0 التي، على التوالي، تبني طوري α–TeO_2 وAg_2TeO_3 البلورية 0. في المنطقة الزجاجية لا يوجد طور بلوري، والتي يمكن أن تعزى إلى وفرة الوحدات المشوهة Q_4^3 التي تبني الطور الزجاجي، ويتم إهمال تركيزات الوحدات Q_4^4 و Q_3^0 في هذه المنطقة. أكدت الصور المجهرية SEM وTEM وأنماط حيود الإلكترون ذات الصلة (EDP) تكوين مجموعات متبلورة في زجاج غنية بـ Ag_2O.

1. Introduction

Tellurite glasses are characterized by their desirable physical properties. They have wide glass formation regions [1–5], extremely high refractive index, high dielectric constant, excellent infrared transmittance, and low melting temperature [6–9]. In addition, TeO_2 is considered as a good agent for crystallization [10].

The structure of tellurite glasses has attracted considerable attention. Various investigators used infrared [2,8,19–22,11–18], Raman [2,15,19,23–25], nuclear magnetic resonance spectroscopies [3,6,26,27] and neutron diffraction [28–31] to study the structural properties of tellurite glasses. Tellurite network is composed of bridging Q_4^4 (TeO_4) and deformed Q_4^3 (TeO_{3+1}) units below 20 mol% alkali oxide. While in the range 20-30 mol% of alkali oxide Q_3^n (TeO_3) were existed with (n=1& 0) having higher non-bridging oxygen atoms (NBOs) in tellurite network and increasing as alkali content increased. The isolated Q_3^0 (TeO_3^{2-}) along with Q_3^1 ($Te_2O_5^{2-}$) structural units are the main formed species at 50 mol% of alkali oxide.

* E-mail: efelagamy@ju.edu.sa, aldhibany@gmail.com

Most of previous studies have focused on the structural species in the modified tellurite in the glassy region for most alkali tellurite glasses [15,26,28,31–33]. Studies on Ag_2O-TeO_2 glasses are so far limited to be considered [34,35]. Therefore, this work is aimed to shed more light on the structural features of Ag_2O-TeO_2 glasses and glass-ceramics and to identify the crystallized phases that formed within the Ag_2O-TeO_2 glass-ceramics.

2. Experimental Methods

Samples with nominal composition $x Ag_2O \cdot (100\text{-}x)TeO_2$ ($0 \leq x \leq 60$ mol%) were prepared by mixing of $AgNO_3$ and TeO_2, in porcelain crucibles. The crucible was firstly transferred into the electric furnace and kept at 300 ^oC for 30 minutes and then it was heated for 10 minutes at a temperature ranged between 800 and 900 ^oC depending on the composition. Finally, the melt was poured and rapidly quenched at room temperature.

The crystallized phases were identified by the (XRD) technique using PANalytical X`Pert PRO XRD system using a Cu K target with secondary monochromator (λ = 1.540 Å). The tube operated at 45 kV- 40 mA. Measurements were made over the range 10° to 70° on 2θ scale. The measurements were carried out at Nano Technology and Advanced Materials Central Lab (NAMCL), Research Institute, Cairo University.

The morphology of the Ag_2O-TeO_2 glasses and glass-ceramics (bulk-fractured surface) was examined using a Scanning Electron Microscope (SEM), model JEOL–JSM–6510LV attached with energy dispersive spectroscopy (EDS) unit, model Oxford–X–Max 20. The size of the formed structural units is examined by Transmission Electron Microscope (TEM), model JEOL JEM-2100 with an electron acceleration voltage of 200 kV. Structural information could be obtained by using electron diffraction patterns (EDP). The measurements were made at the Spectroscopy Unit, Faculty of Science, Mansoura University.

3. Results and Discussion

Local structure of Ag_2O-TeO_2 glasses

Under normal conditions, tellurium oxide cannot form a glass without a modifier [28,36,37]. In both crystalline and amorphous tellurium oxide, the Q_4^4 units are considered as the basic dominant structural units that build the network of the material [22,23,26]. In this case, the tellurium atom is surrounded by four bridging oxygen atoms (BOs). Two BOs are located in axial vertices and the others are in the equatorial positions. In addition, one lone pair of electrons is occupied in a third equatorial site as presented in Fig (1) [2,23].

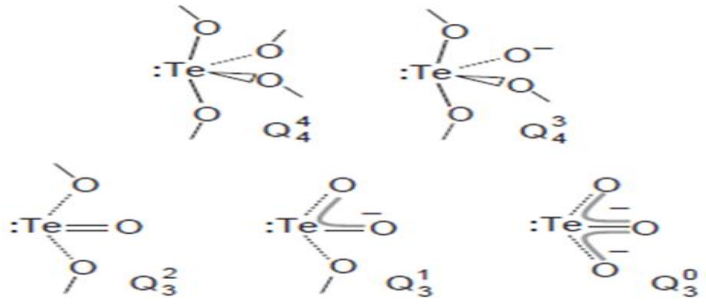

Fig. 1: The tellurium (IV)–oxygen polyhedra found in alkali tellurite crystals and glasses.

The tellurium polyhedral units can be represented by Q_m^n notation, where (*n*) is the number of bridging oxygens (BOs) and (*m*) is the coordination number of the Te atom [38]. It was reported that, the addition of a modifier and/or intermediate oxides into tellurite glasses results in changing Q_m^n unit toward formation of non-bridging oxygen ions (NBOs). These changes are presented schematically in Fig (1).

The mechanism of occurred changes in Q^n_m units that plotted in Fig (1) are explained as following;
1- Firstly, below 10 mol% of modifier oxide such as (Li_2O, Ag_2O, etc.), it is entirely consumed to convert Q^4_4 to Q^1_3 via Q^3_4 units, because the later units are unstable and automatically transformed to (Q^1_3) once [23].

2- Beyond 10 mol% of modifier oxide, it is used to produce either Q^1_3 or Q^0_3 units depending on modifier oxide content [23].

3.1. X-ray diffraction:

XRD patterns of Ag_2O-TeO_2 glasses and glass-ceramics are shown in Figs. (2-a) and (2-b).

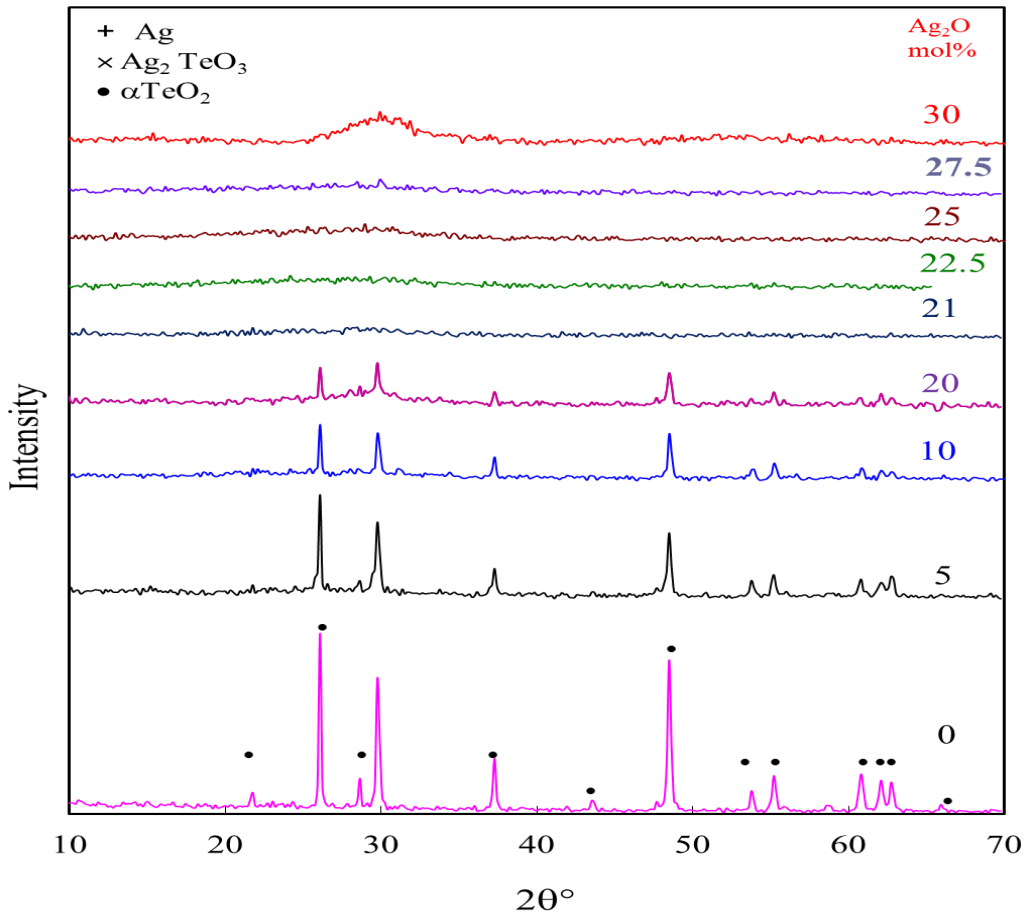

Fig. 2a: X-Ray diffraction pattern for $xAg_2O{\cdot}(100\text{-}x)TeO_2$ glasses and glass-ceramics; ($0 \leq x \leq 30$) mol % Ag_2O containing tellurite glass and glass-ceramics respectively. Numbers at the plots refer to the concentration of Ag_2O (mol %).

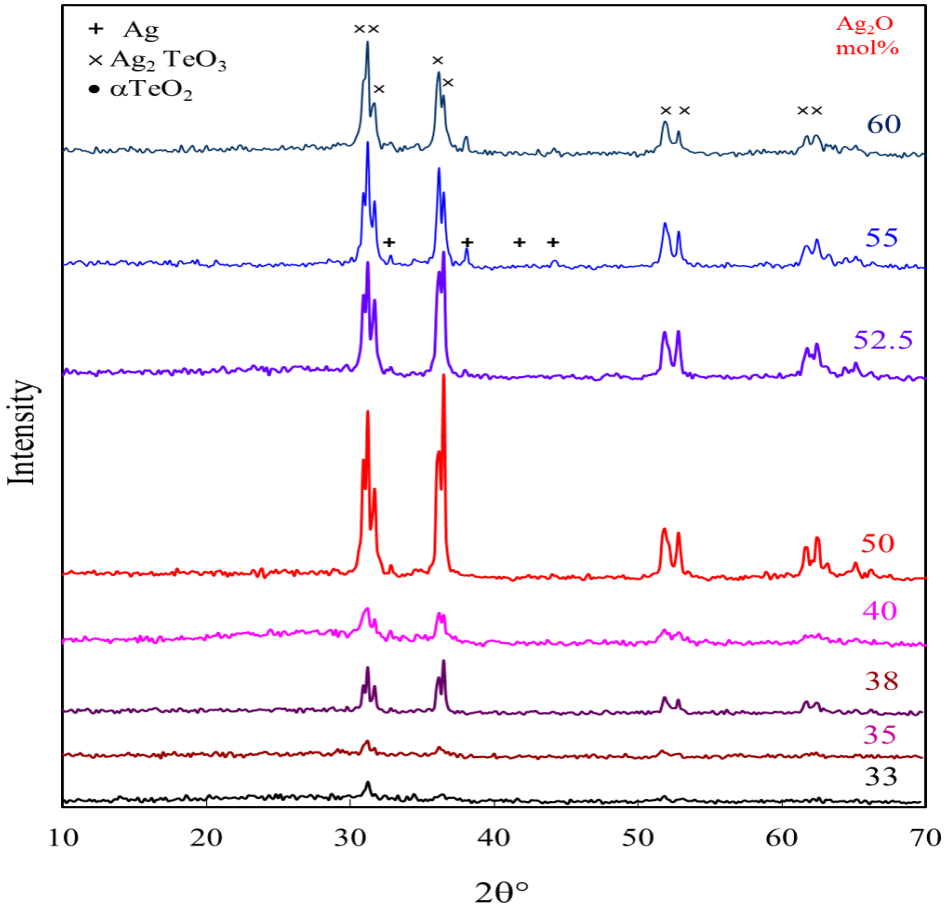

Fig. 2b: X-Ray diffraction pattern for $xAg_2O\cdot(100-x)TeO_2$ glasses and glass-ceramics; ($33 \leq x \leq 60$) mol % Ag_2O containing tellurite glass and glass-ceramics respectively. Numbers at the plots refer to the concentration of Ag_2O (mol %).

The pattern of fused TeO_2 shows many sharp peaks in the region ~ 22–66°. These peaks are related to α-TeO_2 crystalline phase (card 78-1713C). The decrease in intensity of these peaks reflects a decrease in concentration of the Q_4^4 units. This might be accompanied by an increase in the concentration of Q_3^1 and/or Q_3^0 units. The sharp peaks formed in the composition region $0 < x \leq 20$ mol% closely match those related to paratellurite (α-TeO_2) (card number 78-1713C) which is built up by sharing corners of Q_4^4 units. The intensity of these sharp peaks decreases with increasing Ag_2O content which reveals that there is an increase in the disorder of the glass matrix. These sharp peaks disappear completely between 22.5 and 30 mol% Ag_2O, while a broad hump arises at 30 mol% Ag_2O revealing the completely amorphous nature of this composition. In this region the glassy state becomes dominant. Starting from the sample containing 33 mol% Ag_2O, a new sharp peaks-corresponding to Ag_2TeO_3 crystalline phase (card number 83-1779 C) appears with maximum intensity at 50 mol% Ag_2O, where the structure becomes saturated with Ag^+ ions. Beyond 50 mol% Ag_2O, additional small peaks (+) appeared which related to the metallic silver (card number 87-07117).

Changes in the XRD spectral features (intensity and angular position) can be explained on the basis of the following concepts:

1- TeO_2 can be considered as a stable glass former by the effect of the addition of even small quantity of modifiers [39,40].

2- The glass forming ability of tellurium was found to increase with increasing the modifier content up to certain value (30 mol %).

3- For more than 30 mol% of modifier oxide, the glass forming ability is suppressed by forming a new crystalline Ag_2TeO_3 phase which consists of Q_3^0 units. The concentration of the latter increases with increasing modifier content at the expense of TeO_2 [32,39,40].
4- Maximum intensity of the peak related to crystallized Ag_2TeO_3 appears at 50 mol% when R=1, where R is the ratio (Ag_2O/TeO_2), as shown in Fig (2-b). The decrease in the intensity of peaks related to Ag_2TeO_3 for R>1 might be due to the decrease in the TeO_2 content. The presence of excess Ag_2O in such glass-ceramics may be considered as a reason for formation of metallic silver clusters.

Glasses enriched with both Ag_2O and the deshielded Q_3^n units (where n= 0& 1) have increasing ability toward formation of Ag_2TeO_3 crystalline phase and clusters of metallic Ag. This consideration is further supported by the appearance of new sharp diffraction peaks at 2θ = 31.2, 36.68, 51.84, 52.8, 61.76 and 62.52 degree in prepared samples containing 33–60 mol% Ag_2O. The presence of new diffraction peaks at 2θ =38.08 and 44.32 degree at high Ag_2O content (52.5, 55 & 60 mol %) might reflect the inability of the glass matrix to accommodate more of Ag^+ ions. As a result, these excess ions are forced to accumulate in these glasses forming atomic silver clusters. Similar structural changes were assumed by some authors [41,42] in fluorotellurite glasses.

3.2. SEM and EDS techniques

To explore the morphology of the Ag_2O –TeO_2 glasses and glass-ceramics, investigations were performed using SEM. SEM and EDS results agree well with that obtained by the XRD patterns and confirm it. The SEM micrograph of the as-prepared samples of (10, 25, 30, 35 and 50) mol% Ag_2O are shown in Figures 3(a, b, c, d, e & f), respectively. The electron micrographs of the samples with 50 and 55 mol% Ag_2O are shown in Figures 4(a& b) respectively. It is shown that the particle size increases with increasing Ag_2O content in the studied glasses. A. E. Ersundu et.al [43]. have used SEM spectroscopy to study the microstructure of binary CdO-TeO_2, WO_3-TeO_2 and ternary CdO-WO_3-TeO_3 glasses before and after thermal treatment, it was concluded that the dark colored crystallites are due to α-TeO_2 for all glass compositions, while the white colored are rich with WO_3 and CdO and corresponding phases [43]. Figure (3-a) shows an interconnected columns or rods on the surface of the sample with 10 mol% Ag_2O, which corresponds to α-TeO_2 phase as induced from the XDR pattern in Fig. (1-a). These rods are assumed to be due to the α-TeO_2 phase and the background base may represent glassy Ag_2O–TeO_2 matrix. El Agammy et al. [41,42] proposed like these results in the NaF-TeO_2 and PbF_2-TeO_2 glasses and glass-ceramics. The micrograph of the samples containing 25 and 30 mol% Ag_2O are shown in Figs. 3(b & c), respectively. It shows white colored particles with different size dispersed separately through the base matrix. The base matrix is attributed to the modified glassy phase, while the white colored particles are corresponding to Ag_2TeO_3 crystalline phase. (Figs. 3c) shows that the particles in sample of 30 mol% Ag_2O are larger and denser than that of 25 mol%. SEM micrograph of the sample containing 35 mol% Ag_2O is shown in Figs. 3(d& e). Figure (3d) depicts cubic particles having different sizes start growing with fine-grain particles observed on the surface of sample with 30 mol% Ag_2O. Both of fine and cubic-particles might be correspond to Ag_2TeO_3 phase. Figure (3f) depicts formation of columns on the surface of the prepared 50 mol% Ag_2O sample. The cubic particles (Fig. 3d) that produced from fine-grains can be ascribed to the initial stage of the observed rods in the sample containing 50 mol% Ag_2O.

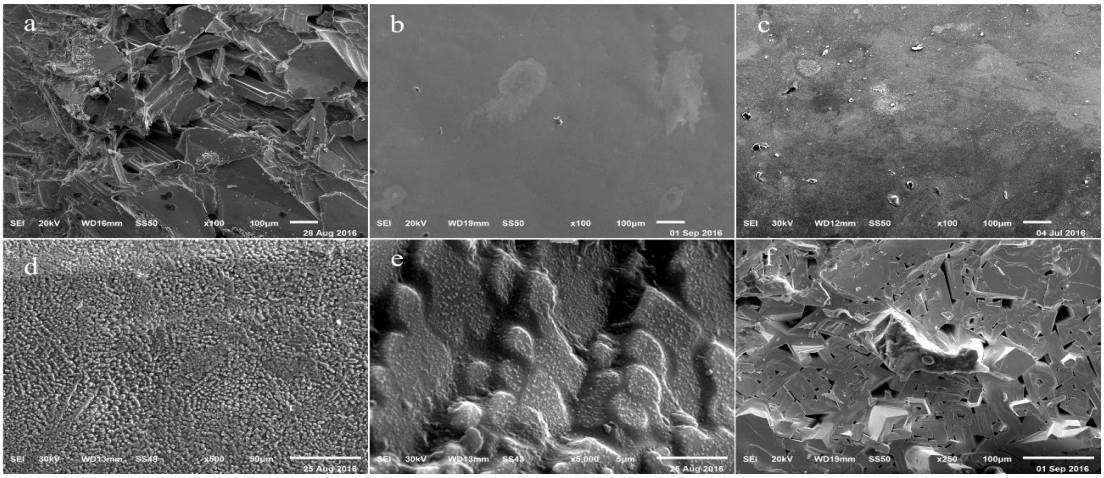

Fig.3: (a, b, c, d, e and f) SEM micrographs on the furcated surface (bulk) for the $xAg_2O{\cdot}(100\text{-}x)TeO_2$ glasses, x=50 and 55 mol%.

The rods have a larger size than that of cubic, revealing to a more ordering (Fig. 2a). The rods might be ascribed to Ag_2OTeO_3 phase as deduced from XRD pattern in Fig. (2-b). The micrograph of 50 mol% Ag_2O (Fig.4a) shows white-colored particles dispersed in the base matrix. These particles are corresponding to metallic Ag. Figure (4b) shows flowers-like crystallites in the prepared $55Ag_2O$-$45TeO_2$ sample.

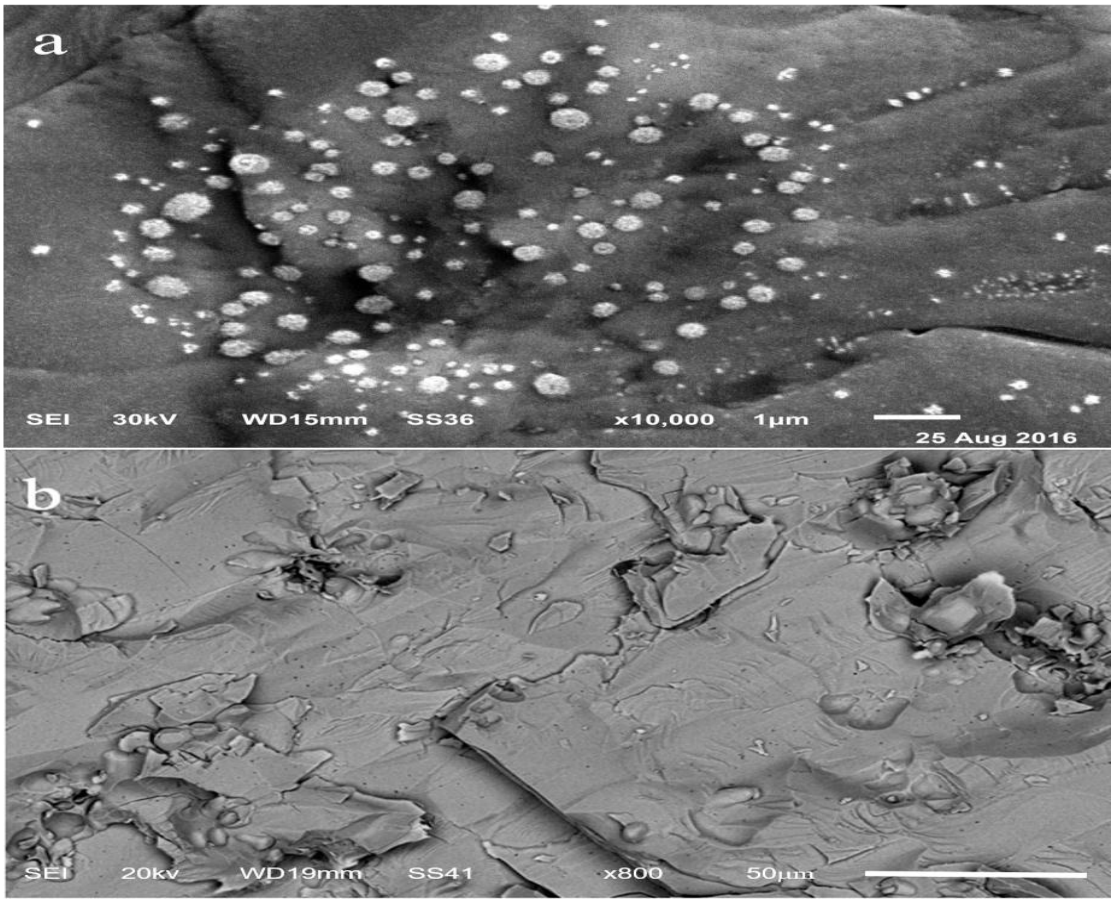

Fig. 4: (a, and b) SEM micrographs on the furcated surface (bulk) for the $xAg_2O{\cdot}(100\text{-}x)TeO_2$ glasses and glass-ceramics, x=50 and 55 mol%.

These flowers seem to be formed as a result of coalescence of white-particles in the sample of 50 mol% Ag_2O. These white flower-like crystallites are corresponding to metallic Ag as deduced from the XRD results.

SEM micrographs reveal a slight increase in particle size when increasing Ag_2O content from 25 to 30 mol% Ag_2O. It becomes clearer when forming the cubic and rods in samples of 35 and 50 % Ag_2O, respectively. It is proposed that, the particle-size is proportional to Ag_2O content. The fine-particles in samples 25 and 30 mol% Ag_2O represent the initial stage of the cubic shape formation, and the latter represents the first stage of rods growth. The glassy phase is predominant in the range $25 \leq Ag_2O \leq 30$ mol%. Whereas, Ag_2TeO_3 phase appears with relatively low intensity at 33 mol% Ag_2O and growths with Ag_2O content until reaching maximum intensity at 50 mol% Ag_2O as in Fig. (2-b), which may be attributed to the formation of the rods respectively as seen in Figs. 3(e-f). So it can be concluded that, development of Ag_2TeO_3 phase within the prepared glass-ceramics can be done by increasing Ag_2O up to 50 mol% Ag_2O, where the structure becomes saturated with Ag_2TeO_3 phase and excess added of Ag_2O is precipitated inside the network as metallic silver as shown in Figs. (2-b) and (4-b).

EDS spectra of Ag_2O –TeO_2 glasses and glass-ceramics containing 10, 30, 50 and 55 mol% of Ag_2O are shown in Fig. 5. At 10, 30 mol % of Ag_2O, the increase in peak intensity of silver compared to that of Te with Ag_2O content supports the XRD results. The intensity of the Ag peak may refer to concentration of Ag^+ ions in these NBOs units. However, at higher concentrations (≥ 50 mol% Ag_2O), the structure may become saturated with NBOs units containing Ag^+ ions and the excess of Ag_2O is precipitated as metallic silver.

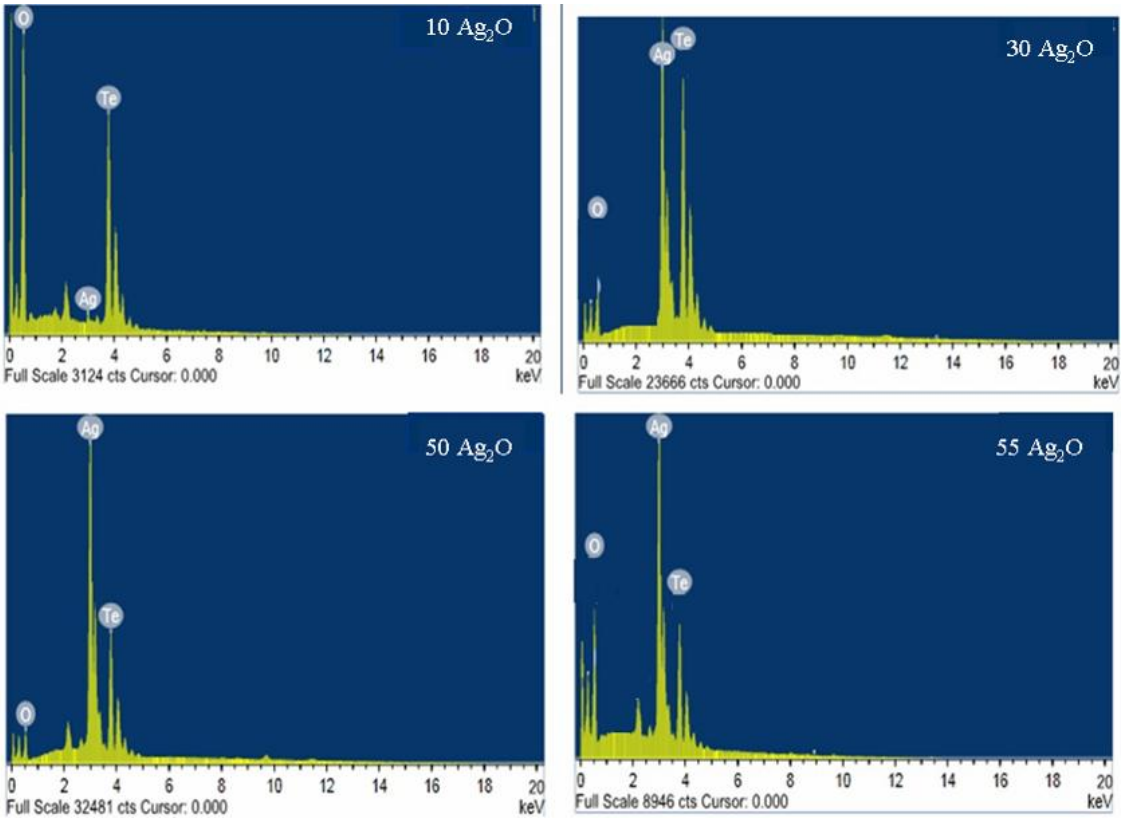

Fig. 5: EDS spectrum of the $xAg_2O.(100-x)TeO_2$ glasses and glass-ceramics, x=10, 30, 50 and 55 mol% Ag_2O.

3.3. TEM and EDP Techniques

The TEM and EDP results agree with those obtained by the SEM, EDS and XRD for selected samples. The TEM micrographs and electron diffraction pattern (EDP) for samples with 10, 30, 35 and 50 mol%

Ag_2O are shown in Fig. 6 (a, b, c& d) respectively. The TEM micrograph of 10 mol% Ag_2O sample shows rods along with fine-grains of (2-3) nm in size (Fig 6a).

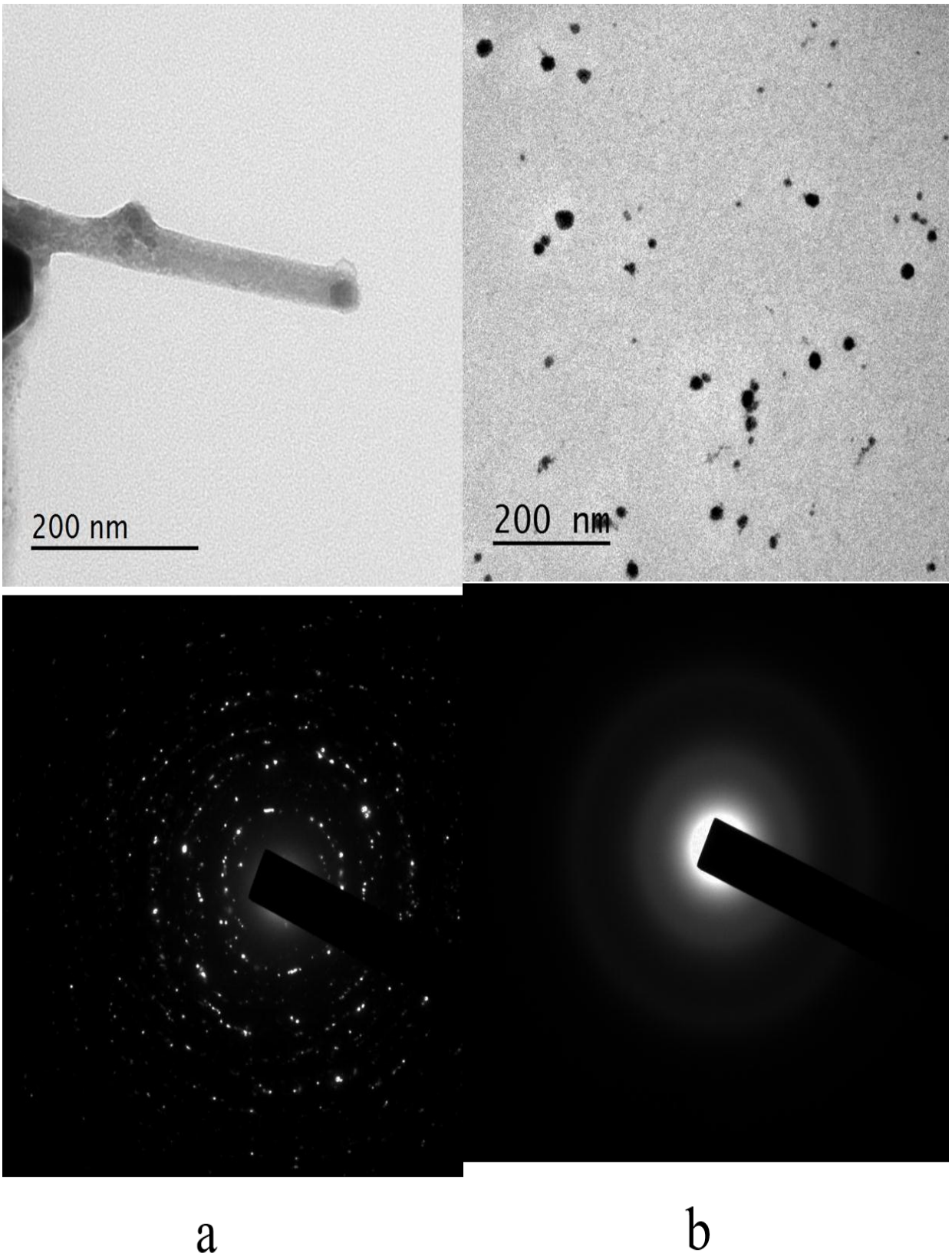
200 nm
200 nm
a
b

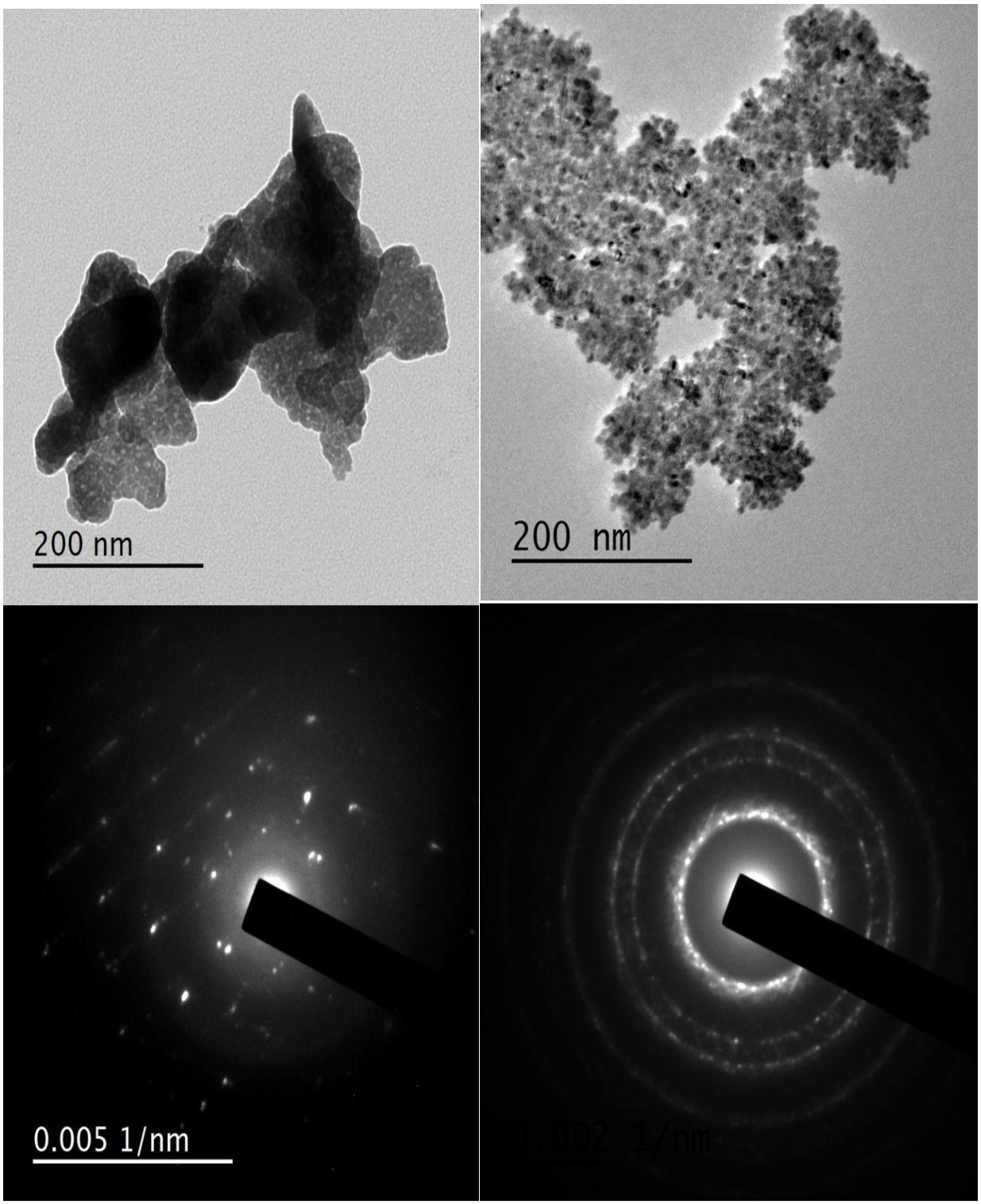

Fig.6: (a, b, c and d), TEM images and the EDP of TeO_2 glass containing 10, 30, 35 and 50 mol% Ag_2O respectively.

The EDP pattern shows more ordering structure as shown in (Fig. 6a). For the sample with 30 mol% Ag_2O, the size of the formed particles was found to vary from 11 to 50 nm and the distribution of these particles in the network is randomly as presented in Fig. 6b. The diffused circles in the EDP patterns are characteristic of the amorphous matrix at Ag_2O = 30 mol% that mainly might be Ag_2O –TeO_2 phase. The TEM micrograph of the sample with 35 mol% Ag_2O shows that, these fine-particles are aggregated in large size (black zones) through the network (Fig.

6c), where the ordering increases due to formation of these zones with a large size as deduced from the EDP pattern (Fig. 6c). These fine particles become more accumulated in case of 50 mol% Ag_2O compared to that of 35 mol%, leading to more order as seen in Figs. (2a& 6d).

4. Conclusions

The samples from $x Ag_2O \cdot (100-x) TeO_2$ ($0 \leq x \leq 60$ mol%) system were prepared and investigated through, XRD, SEM, EDS and TEM techniques. There are two mainly crystalline phases, α-TeO_2 and Ag_2TeO_3. However, the crystallinity decreases with the Ag_2O content below 20 mol% and disappears completely in the range ($20< Ag_2O \leq 30$) mol%, it returns to increase with the Ag_2O content beyond 30 mol%. Q_4^4 and Q_3^0 units that, respectively, built up crystalline α-TeO_2 and Ag_2TeO_3 phases are decreased and increased with addition of Ag_2O below and beyond 30 mol% Ag_2O, respectively. Disappearing of the formed crystalline phases in the glassy region might be due to abundance of the deformed Q_4^3 units, related to the glassy phase, and the concentrations of both Q_4^4 and Q_3^0 units are neglected.

5. References

[1] K. Ramesh, S. Asokan, K.S. Sangunni, E.S.R. Gopal, Glass formation in germanium telluride glasses containing metallic additives, J. Phys. Chem. Solids. 61 (2000) 95–101.
[2] Q.J. Rong, A. Osaka, T. Nanba, J. Takada, Y. Miura, Infrared and Raman spectra of binary tellurite glasses containing boron and indium oxides, J. Mater. Sci. 27 (1992) 3793–3798.
[3] S. Sakida, S. Hayakawa, T. Yoko, 125Te, 27Al, and 71Ga NMR study of M2O3–TeO2 (M= Al and Ga) glasses, J. Am. Ceram. Soc. 84 (2001) 836–842.
[4] H. Nasu, O. Matsushita, K. Kamiya, H. Kobayashi, K. Kubodera, Third harmonic generation from Li2OαTiO2αTeO2 glasses, J. Non. Cryst. Solids. 124 (1990) 275–277.
[5] S. Tanabe, K. Hirao, N. Soga, Upconversion fluorescences of TeO2-and Ga2O3-based oxide glasses containing Er3+, J. Non. Cryst. Solids. 122 (1990) 79–82.
[6] S. Sakida, S. Hayakawa, T. Yoko, 125Te NMR study of MO-TeO2 (M= Mg, Zn, Sr, Ba and Pb) glasses, J. Ceram. Soc. Japan. 107 (1999) 395–402.
[7] J.E. Stanworth, Tellurite glasses, Nature. 169 (1952) 581.
[8] H. Bürger, W. Vogel, V. Kozhukharov, IR transmission and properties of glasses in the TeO2-RnOm, RnXm, Rn (SO4) m, Rn (PO3) mandB2O3] systems, Infrared Phys. 25 (1985) 395–409.
[9] M.J. Redman, J.H. Chen, Zinc tellurite glasses, J. Am. Ceram. Soc. 50 (1967) 523–525.
[10] I. Avramov, G. Guinev, A.C.M. Rodrigues, Thermal analysis of Li2O TeO2 glass, J. Non. Cryst. Solids. 271 (2000) 12–17.
[11] M. Arnaudov, V. Dimitrov, Y. Dimitriev, L. Markova, Infrared-spectral investigation of tellurites, Mater. Res. Bull. 17 (1982) 1121–1129.
[12] Y. Dimitriev, V. Dimitrov, M. Arnaudov, IR spectra and structures of tellurite glasses, J. Mater. Sci. 18 (1983) 1353–1358.
[13] M. Arnaudov, Y. Dimitriev, V. Dimitrov, M. Dimitrova-Pankova, C.H. Petkov, IR-spectral investigation of glasses of the TeO22□ GeO2 system, Mater. Chem. Phys. 21 (1989) 215–222.
[14] T. Yoko, K. Kamiya, K. Tanaka, H. Yamada, S. Sakka, Glass-forming region and structure of oxyhalide tellurite glasses containing LiX (X= F and Br) and Li2O, J. Ceram. Soc. Japan. 97 (1989) 289–294.
[15] J. Heo, D. Lam, G.H. Sigel Jr, E.A. Mendoza, D.A. Hensley, Spectroscopic analysis of the structure and properties of alkali tellurite glasses, J. Am. Ceram. Soc. 75 (1992) 277–281.
[16] P. Armand, P. Charton, New ternary tellurite glasses: TeO2-WO3-Sb2O4 and TeO2-WO3-Ga2O3, Phys. Chem. Glas. 43 (2002) 291–295.
[17] A.A. El-Moneim, DTA and IR absorption spectra of vanadium tellurite glasses, Mater. Chem. Phys. 73 (2002) 318–322.

[18] M.A. Frechero, O.V. Quinzani, R.S. Pettigrosso, M. Villar, R.A. Montani, IR absorption spectra of lithium and silver vanadium–tellurite based glasses, J. Non. Cryst. Solids. 353 (2007) 2919–2925.
[19] R.C. Lucacel, I.C. Marcus, I. Ardelean, O. Hulpus, Structural studies of copper doped 2TeO2–PbO–Ag2O glass by FT-IR and Raman spectroscopies, Eur. Phys. Journal-Applied Phys. 51 (2010).
[20] P.G. Pavani, K. Sadhana, V.C. Mouli, Optical, physical and structural studies of boro-zinc tellurite glasses, Phys. B Condens. Matter. 406 (2011) 1242–1247.
[21] P.G. Pavani, S. Suresh, V.C. Mouli, Studies on boro cadmium tellurite glasses, Opt. Mater. (Amst). 34 (2011) 215–220.
[22] D. Muñoz-Martín, M.A. Villegas, J. Gonzalo, J.M. Fernández-Navarro, Characterisation of glasses in the TeO2–WO3–PbO system, J. Eur. Ceram. Soc. 29 (2009) 2903–2913.
[23] T. Sekiya, N. Mochida, A. Ohtsuka, M. Tonokawa, Raman spectra of MO1/2TeO2 (M= Li, Na, K, Rb, Cs and Tl) glasses, J. Non. Cryst. Solids. 144 (1992) 128–144.
[24] T. Sekiya, N. Mochida, A. Soejima, Raman spectra of binary tellurite glasses containing tri-or tetra-valent cations, J. Non. Cryst. Solids. 191 (1995) 115–123.
[25] Y. Himei, A. Osaka, T. Nanba, Y. Miura, Coordination change of Te atoms in binary tellurite glasses, J. Non. Cryst. Solids. 177 (1994) 164–169.
[26] S. Sakida, S. Hayakawa, T. Yoko, Part 2.125 Te NMR study of M2O–TeO2 (M= Li, Na, K, Rb and Cs) glasses, J. Non. Cryst. Solids. 243 (1999) 13–25.
[27] S. Sakida, S. Hayakawa, T. Yoko, Part 1. 125Te NMR study of tellurite crystals, J. Non. Cryst. Solids. 243 (1999) 1–12.
[28] S. Neov, I. Gerasimova, V. Kozhukharov, M. Marinov, The structure of glasses in the TeO2-P2O5 system, J. Mater. Sci. 15 (1980) 1153–1166.
[29] Y. Toshinobu, Neutron diffraction study on the structure of pure $ TeO_2 $ glass, J. Korean Cryst. Growth Cryst. Technol. 5 (1995) 189–196.
[30] M.A.P. Silva, Y. Messaddeq, S.J.L. Ribeiro, M. Poulain, F. Villain, V. Briois, Structural studies on TeO2–PbO glasses, J. Phys. Chem. Solids. 62 (2001) 1055–1060.
[31] H. Niida, T. Uchino, J. Jin, S.-H. Kim, T. Fukunaga, T. Yoko, Structure of alkali tellurite glasses from neutron diffraction and molecular orbital calculations, J. Chem. Phys. 114 (2001) 459–467.
[32] A. Šantić, A. Moguš-Milanković, K. Furić, M. Rajić-Linarić, C.S. Ray, D.E. Day, Structural properties and crystallization of sodium tellurite glasses, Croat. Chem. Acta. 81 (2008) 559–567.
[33] S.L. Tagg, R.E. Youngman, J.W. Zwanziger, The structure of sodium tellurite glasses: Sodium cation environments from sodium-23 NMR, J. Phys. Chem. 99 (1995) 5111–5116.
[34] K. Kato, T. Hayakawa, Y. Kasuya, P. Thomas, Influence of Al2O3 incorporation on the third-order nonlinear optical properties of Ag2O–TeO2 glasses, J. Non. Cryst. Solids. 431 (2016) 97–102.
[35] Y. Iwadate, M. Suzuki, T. Hattori, K. Fukushima, S. Nishiyama, M. Misawa, T. Fukunaga, K. Itoh, Evolution of local structure in Ag2O–TeO2 glasses with addition of Ag2O analyzed by pulsed neutron diffraction and Raman spectroscopy, J. Alloys Compd. 389 (2005) 229–233.
[36] L.M.S. El-Deen, M.S. Al Salhi, M.M. Elkholy, IR and UV spectral studies for rare earths-doped tellurite glasses, J. Alloys Compd. 465 (2008) 333–339.
[37] S.S. Babu, P. Babu, C.K. Jayasankar, A.S. Joshi, A. Speghini, M. Bettinelli, Luminescence and optical absorption properties of Nd3+ ions in K--Mg--Al phosphate and fluorophosphate glasses, J. Phys. Condens. Matter. 18 (2006) 3975.
[38] J.C. McLaughlin, S.L. Tagg, J.W. Zwanziger, D.R. Haeffner, S.D. Shastri, Structure of tellurite glass: A combined NMR, neutron diffraction, and X-ray diffraction study, J. Non. Cryst. Solids. 274 (2000) 1–8.
[39] K. Tanaka, T. Yoko, H. Yamada, K. Kamiya, Structure and ionic conductivity of LiClLi2OTeO2 glasses, J. Non. Cryst. Solids. 103 (1988) 250–256.
[40] K.B. Kavaklıoğlu, S. Aydin, M. Çelikbilek, A.E. Ersundu, The TeO2-Na2O System: Thermal Behavior, Structural Properties, and Phase Equilibria, Int. J. Appl. Glas. Sci. 6 (2015) 406–418.

[41] E.F. El Agammy, H. Doweidar, K. El-Egili, R. Ramadan, M. Jaremko, A.-H. Emwas, Structure of NaF–TeO2 glasses and glass-ceramics, Ceram. Int. 46 (2020) 18551–18561.
[42] E.F. El Agammy, a, H. Doweidar, K. El-Egili, Structure of PbF2–TeO2 glasses and glass-ceramics, Mater. Res. Technol, 9(3), 4016-4024.
[43] A.E. Ersundu, M. Çelikbilek, S. Aydın, A review of scanning electron microscopy investigations in tellurite glass systems, FORMATEX. (2012) 1105–1114.